JOURNAL OF MATERIALS SCIENCE **40** (2005) 4173–4179

Dynamic properties characterization of metastable Al/Ti composites

N. SRIKANTH, LOU KUM HOONG, M. GUPTA
Department of Mechanical Engineering, National University of Singapore, 9 Engineering Drive 1, Singapore, 117576
E-mail: mpegm@nus.edu.sg

A new idea of using stiffer metallic reinforcement, such as titanium, in a ductile metallic matrix, such as aluminium, to enhance the dynamic properties (viz., stiffness and damping) is successfully attempted. The study focuses on the relationship between the stiffness and the damping capability of the aluminium matrix with the weight percentage of titanium added to it. Results of this study show that addition of about 3.2, 6 and 7.5 wt% of titanium increases the overall damping capacity of the Al matrix by 6, 17 and 24%, respectively. Particular emphasis is placed to rationalize the increase in damping in terms of the increase in dislocation density and presence of plastic zone at the matrix-particulate interface.

1. Introduction

Accumulation of vibration energy increases the vibration amplitude in a dynamic mechanical system. Hence damping, which refers to the dissipation of energy to the surrounding environment by a reversible microstructural movement or an irreversible thermoelastic process inside the material during mechanical vibration, is generally sorted as a solution in the design [1]. Parallel to this option, stiffness can be increased as it refers to the capacity of a mechanical system to sustain loads without excessive changes in its geometry (generally called deformations). Thus materials with increased stiffness and damping property are actively sought for the design of dynamic mechanical systems such as in spacecrafts, semiconductor equipments and robotics.

Studies have demonstrated that it is possible to achieve significant improvements in the stiffness and damping behavior of metal matrix composites (MMCs), by incorporating certain types of dispersoids in the metal matrix [1–4]. Aluminium based formulations are one such category of light weight materials that has the capability to exhibit such properties especially when it is unified with stiffer ceramic particulates [1, 2]. In related studies, it has been shown that the addition of ceramic particulates to the aluminium matrix assists in improving damping properties of the overall composite [3]. Additionally, the authors presented the idea of interconnected metallic reinforcements that also resulted in the significant increase in damping and stiffness of the composite material [4]. Investigation related to machinability of MMCs has shown that the presence of hard ceramic phase decreases the tool life of cutting tools drastically [5]. Hence the idea of dis-continuous stiffer metallic phase in a ductile metallic phase adopted in the present study may enhance the machinability of this new MMC. The results of the literature search, however, reveal that no attempt has been made to investigate such metallic reinforcements addition on the damping behavior of aluminium.

Previous studies of Gupta *et al*. [6] has shown that titanium dissolves in aluminium at high temperatures and forms intermetallics with Al following solidification. The synthesis and processing of such material is extremely challenging due to the ability of Ti to raise the melting temperature of Al and extreme reactive nature of molten Al-Ti mixture. In order to avoid these limitations, Ti was subjected to surface modification so that it stays as elemental-Ti, mostly, following solidification. In addition, titanium being a stiffer material with a elastic modulus of 120 GPa, has a higher melting point of 1667°C, and a hardness of 90 HV, and hence when left un-dissolved in molten aluminum matrix by proper surface modification on the particle surface, it can result in reinforcing the ductile Al matrix, which has a melting point of 660.3°C, elastic modulus of 72.2 GPa and a hardness of 15 HV [7]. But, in terms of density, Ti is heavier than Al by 1.6 times which can make the composite heavier, but when added in smaller volume fraction this effect may not be a significant factor in the design. Hence the primary objective of this investigation was to investigate the energy dissipation of aluminium containing variable amounts of pure Ti phase.

2. Materials and processes

In this study, pure Al (purity > 99.7%) was the base metal and titanium powders with an average size of 19 ± 9 μm were used as the starting materials. To prevent Ti dissolution in Al, the Ti particle's surface was modified by preheating at 400°C for an hour in a ceramic container to produce a surface oxide layer and

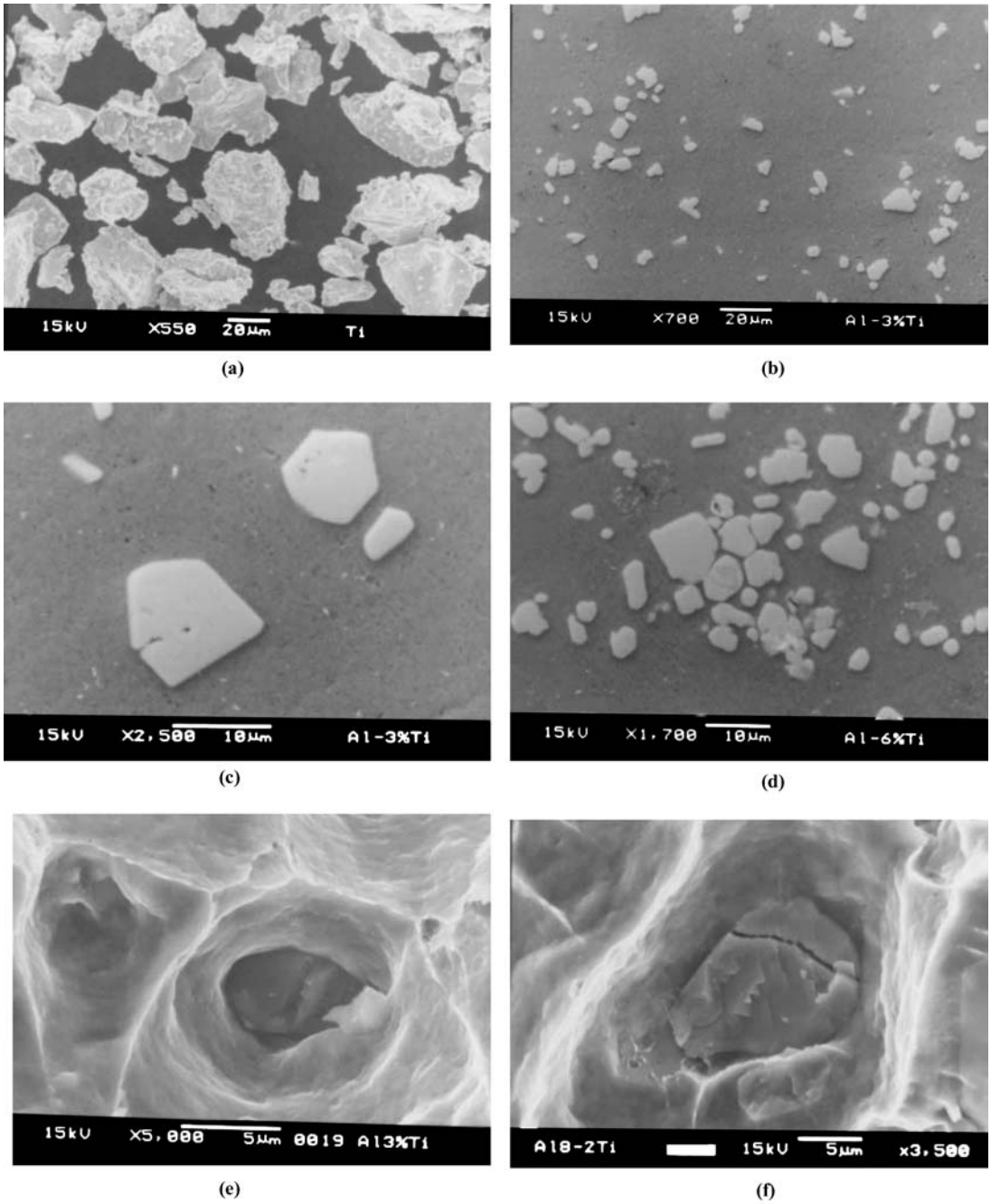

Figure 1 SEM micrographs showing (a) pure Ti particulates (b) reinforcement distribution in Al-3.3%Ti (c) good interfacial integrity of the reinforcement exhibited in Al-3.3%Ti (d) Typical clustering of particles in Al-6%Ti (e) fractograph exhibiting particulate debonding in Al-3.3% Ti (f) fractograph exhibiting particulate breakage in Al-7.5% Ti.

then added to the molten aluminum melt (750°C) and mechanically stirred using a zirtex-coated stirrer. The resultant slurry was allowed to flow out of the crucible and was atomized using argon gas jets positioned at a distance of ∼215 mm from the pouring point and deposited into a metallic substrate 500 mm from the disintegrating point.

X-ray diffraction was conducted to verify the presence of the reinforcement and also to detect the presence of any reaction phases that might have formed during the casting process. The lattice d-spacing corresponding to the different Bragg angles obtained from scanning each sample were matched with the standard values. Table lists the X-ray diffraction results confirming the presence of elemental Ti along with other Al-Ti and Ti-O related phases.

Fig. 1a shows the typical SEM micrograph of the Ti particulates used as reinforcement. The processing parameters were controlled so as to allow only partial reaction of titanium with the metallic melt. Three composite ingots with 3.3, 6 and 7.5 equivalent of titanium in weight percentage were extruded. Scanning electron microscopy and energy dispersive spectrometer (EDS) studies were conducted to establish the presence of titanium and Ti-rich phases. The results of microstructural characterization of the MMC specimens obtained using image analysis and the density measurements are listed in Table I. Fig. 1b to d shows typical SEM micrographs, which illustrates the microstructural and fracture characteristics of various composite samples.

The coefficient of thermal expansion of extruded composite samples was determined using

TABLE I Results of the microstructural and thermo-mechanical characterization

Ti weight (%)	Density (g/cm^3)	Ti particulate size (μm)	Ti particulate aspect ratio	Exp. mean CTE (10^{-6}/°C)	Matrix* hardness (HV)	Interface* hardness (HV)
0.0	2.701	–	–	25.246	31.9 ± 0.52	–
3.3	2.732	4.7 ± 2.2	1.2 ± 0.3	25.260	34.0 ± 0.60	40.4 ± 0.92
6	2.756	3.3 ± 1.4	1.2 ± 0.3	23.065	43.4 ± 2.04	49.9 ± 0.83
7.5	2.767	5.6 ± 2.9	1.2 ± 0.3	22.651	39.6 ± 0.93	49.7 ± 0.36

*Denotes average value of three Vickers microhardness test results.

thermal-mechanical analyzer and the results are listed in Table I. The micro-hardness measurements were conducted on the monolithic and reinforced samples using a digital micro-hardness tester. In the composite specimens, the microhardness measurements were made on the aluminium matrix and the interfacial zone, which are listed in Table I. It may be noted that interfacial zone refers to the annular region around the reinforcement characterized by high dislocation density originating due to the difference in coefficient of thermal expansion of the matrix and reinforcement. It may be noted that the average values of microhardness of the samples increased up to 6% Ti sample and marginally reduced for 7.5% Ti sample. The results also revealed that the interface hardness in all the three composite samples was higher when compared to the matrix hardness and its value also follows the similar trend as that of the matrix hardness.

Fractographic studies using scanning electron microscopy (SEM) were also conducted on the tensile fractured surfaces of monolithic aluminum and its composite samples to provide an insight into the various possible fracture mechanisms operating during the tensile loading of the samples. Fig. 1e and f shows the typical particle fracture and debonding failure observed in the various tensile fractured surfaces of the composite samples.

3. Damping measurement method

The impact-based "Free-Free" or "Suspended" beam method was performed based on the ASTM C1259-98 standard [8]. Description of the experimental setup is described in reference [4]. The receptance frequency response function (FRF) '$\alpha(\omega)$', which is the ratio between displacement response to the applied impact force, was plotted as a nyquist plot corresponding to the resonance condition [9]. Using least square technique a circle was fit and based on hysterically damped vibrating system the circle diameter can be shown to be inversely dependent on the damping coefficient. Fig. 2 shows typical circle fit plots of the monolithic sample and the composite samples containing 3.3, 6 and 7.5 wt% of Ti. The exact location and determination of the natural frequency and the corresponding damping factor 'η' was calculated using frequency spacing technique [9]. Fig. 3 shows the typical circle plot from which two points are selected for damping loss factor calculation, denoted as point a and b corresponding to frequencies ω_a and ω_b, respectively, which are lesser and greater than the natural frequency ω_n, respectively. Thus, the damping factor η can be expressed using the angles shown in Fig. 3, as follows [4]:

$$\eta = \frac{\omega_a^2 - \omega_b^2}{\omega_n^2} \frac{1}{\tan(\Delta\theta_a) + \tan(\Delta\theta_b)} \tag{1}$$

Based on the ASTM standard C1259-98 [8], the dynamic elastic modulus E is expressed as Equation 2, in terms of fundamental natural frequency ω_n, in rad/sec, mass of the bar (m), in grams, and the beam dimensions, viz., diameter (d) and length (L), in mm. The error due to finite diameter of the bar and the Poisson's ratio of the material is accounted by the correction factor C. For bars with slenderness ratio ($k = L/d$) greater than 20, it is given by $(1 + 4.939/k^2)$.

$$E = 0.04069\left(\frac{L^3}{d^4}\right)C\left(m\omega_n^2\right) \tag{2}$$

4. Results and discussion

The suspended beam experimental method was found to be highly repeatable and was nondestructive. The circle-fit approach was found to be efficient in determining the damping factor from the suspended beam's FRF data. Using this approach, the damping factor of pure aluminium was found to be 0.00322 ± 0.0005, which can be compared with axial damping measurements of Lazan that range from 0.0003 to 0.006 [10]. Literature review shows damping capacity of a material depends on operational frequency and strain amplitude and the difference in the material processing method which results in different microstructure in terms of grain size and shape [1, 10].

Al alloys containing Ti as primary alloying element have proven to be suitable for high temperature and high stress conditions. Such addition results in increase in melting temperature of aluminium (for example additon of 10 wt% of Ti raises the melting point from ~660°C to ~ 1200°C), increases chemical reactivity of the molten mixture and forms many phases, among which three types of phases (viz., Ti_3Al, TiAl and Al_3Ti) are seen to be ordered intermetallic phases [11]. Under equilibrium conditions the upper bound of Ti that can be completely dissolved in molten Al at 750°C should not exceed 0.33 wt%. Hence Gupta *et al.* [12] devised a new generation Al-Ti material by preseving the elemental Ti in the Al matrix. This was done by controlling the residency time of Ti in molten Al and by modifying the surface characteristics of Ti powders with a heat treatment that produces an additional oxide layer on the particle surface. Such a

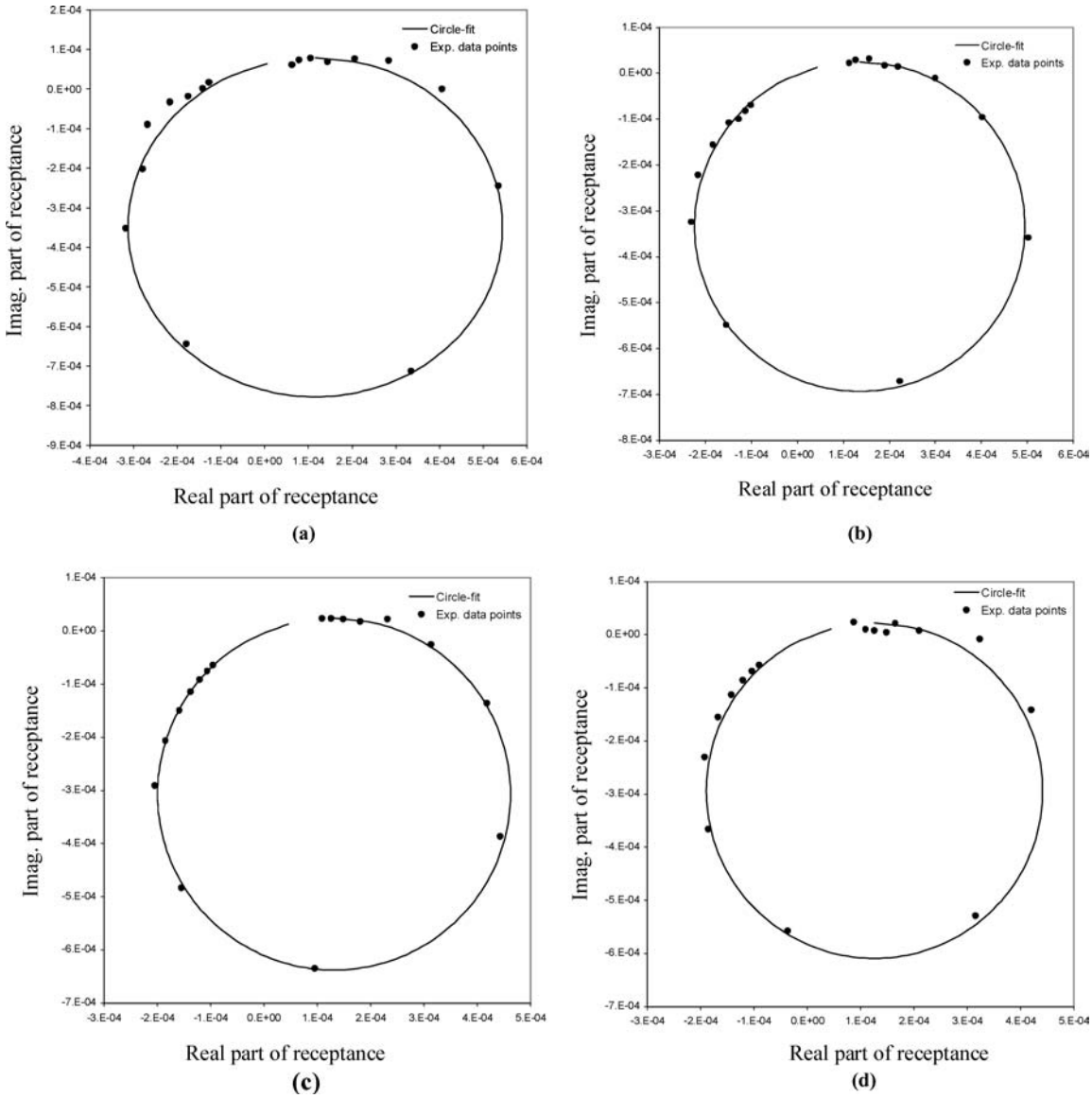

Figure 2 Circle-fit plot of raw FRF data of: (a) the pure Al sample (b) the Al-3.3%Ti sample (c) the Al-6%Ti sample and (d) the Al-7.5%Ti sample.

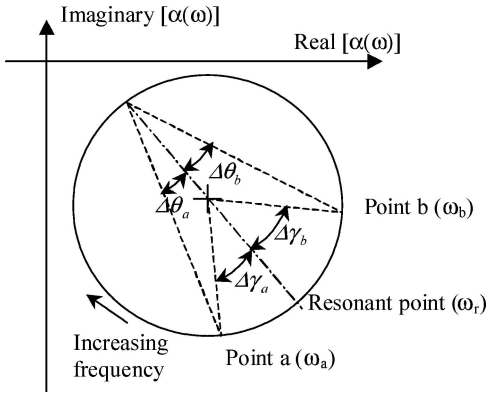

Figure 3 Use of the natural frequency and two data points to derive the damping factor.

surface modification method was adopted in the present study.Computation of the gibbs free energy of formation(ΔG_f), corresponding to a temperature of 750°C, using the published results of reference [13] shows that for Ti_3Al, TiAl and Al_3Ti the ΔG_f magnitudes are −22.77, −20.26 and −29.75 KJ/mol, respectively. Hence growth of Al_3Ti is found to be more favorable than the other phases. At temperatures below melting point of aluminium (660°C), Al diffuses predominantly and the growth of Al_3Ti intermetallic occurs exclusively on Ti-rich side through a peritectic reaction [13]. In the present study, XRD results (see Table II) confirms the presence of Al_3Ti for the present material process condition in all the composite samples. Close inspection

TABLE II X-ray diffraction results obtained from the preheated Ti powder and the extruded specimens

	Number of matching peaks			
Material	Ti (400°C)	Al-3.3% Ti	Al-6% Ti	Al-7.5% Ti
Ti	8	1	1	1
Ti_2O_3	1	0	0	0
TiO	0	0	1	1
TiO_2	0	1	1	1
Al	0	4	4	4
Al_3Ti	0	1	2	1
Total number of peaks	9	7	9	8

of the particle-matrix interface at high magnification in all the three different composites investigated, showed good Ti-Al interfacial bonding with limited interfacial reaction (see Fig. 1c). The particle-matrix interfacial integrity assessed in terms of interfacial debonding and presence of voids was found to be good in the composite sample. XRD results listed in Table II confirm the metastable nature of Al-Ti materials using DMD method with the presence of titanium as elemental Ti.

In general, uniform distribution of Ti particulates and its intermetallic phases in the metal matrix was seen in all the composite samples (see Fig. 1b). Thus an isotropic material behavior can be expected in all the composite samples, from a global perspective. Occasional particulate clustering was also seen from the cross-sectional study (see Fig. 1d). In the present study, fracture surface of the tensile test specimens for the three different MMC samples showed fracture path passing through the Ti particle, confirming a reasonably good interfacial bond at the matrix-reinforcement interface (see Fig. 1e and f). Under this situation, a semi-coherent or incoherent interface exists at the atomistic level.

Material damping is related to the time-dependent elastic behavior of materials. Metallic materials respond to an applied load not only by an instantaneous elastic strain $\varepsilon_{\text{elastic}}$ that is time independent, but also by a strain lagging behind the applied load, which is time dependent in nature. Therefore the overall strain ε is the sum of elastic part $\varepsilon_{\text{elastic}}$ and the anelastic part $\varepsilon_{\text{anelastic}}$ as described in Equation 3, while the variation in the anelastic part of the strain for the loading and the unloading part can be expressed as $\varepsilon_{\text{anelastic-loading}}$ and $\varepsilon_{\text{anelastic-unloading}}$ by Equations 4 and 5, respectively, as follows [10]:

$$\varepsilon = \varepsilon_{\text{elastic}} + \varepsilon_{\text{anelastic}} \tag{3}$$

$$\varepsilon_{\text{anelastic-loading}} = \varepsilon_{\text{initial}}[1 - \exp(-t/\tau)] \tag{4}$$

$$\varepsilon_{\text{anelastic-unloading}} = \varepsilon_{\text{initial}}[\exp(-t/\tau)] \tag{5}$$

where $\varepsilon_{\text{initial}}$ is the initial strain, t is the time and τ is the relaxation constant which signifies the intrinsic energy dissipated within the material. Hence such a strain response under a sinusoidally varying applied stress σ with a frequency ω, results in a hysterisis loop, which represents the energy dissipated in one loading cycle ΔW and can be mathematically represented as follows:

$$\Delta W = \oint \sigma.\mathrm{d}\varepsilon \tag{6}$$

The maximum strain energy W can be shown to be:

$$W = \int_{\omega t=0}^{\omega t=\pi/2} \sigma.\mathrm{d}\varepsilon \tag{7}$$

The damping loss factor η, which is the ratio of ΔW versus W, can be shown to be a function of the time constant τ based on Equations 3–5. Furthermore, the stiffness of the material E^* which is the ratio of stress versus strain at any given time instant can be shown to be a complex number due to the anelastic behavior based on the above equations (i.e. from (3) to (7)) and hence related to the measured modulus and damping loss factor, as follows:

$$E^* = \frac{\sigma}{\varepsilon} = E' + iE'' = E'\left(1 + i\frac{c\omega\tau}{1+\omega^2\tau^2}\right) = E'(1 + i\eta) \tag{8}$$

where E' is the storage modulus, E'' is the loss modulus, c is a constant and i is the complex number ($\sqrt{-1}$).

It is interesting to note that for both good and bad interfacial bonding condition between the Ti particle and the metal matrix, the overall damping characteristics increases in a MMC due to different damping mechanisms while the stiffness improves only for good interfacial bonding. From Equation 8 one can conclude that stiffness and damping capacity of a material are interrelated and hence it is a challenge to improve both in a composite material. Table III lists the damping loss factor and the elastic modulus of the monolithic sample and the three Al-Ti samples. Comparison against the monolithic material condition shows that addition of Ti in the Al matrix increases the overall damping capacity as well as stiffness of the composite. In addition, this improvement steadily increases with Ti weight percentage. Hence it is convincing that the idea of stiffer metallic reinforcements in a ductile matrix serves a two pronged advantage when it is tailored for vibration suppression application.

This increase in the elastic modulus with increase in weight percentage of reinforcement can be attributed to the higher elastic modulus of Ti, which is reported to be about 120 GPa [7] as compared to the monolithic Al sample's elastic modulus value of 68.39 GPa, based on the present study (see Table III). In addition, presence of brittle Al-Ti based intermetallic phases and the oxide phases in the metallic matrix are expected to increase the overall composite's stiffness, due to their higher stiffness compared to the parent materials. In a previous study [2] the authors have used various theoretical models such as the Shear Lag model, Halpin-Tsai model and the Eshelby model to explain such an increase in the MMC's stiffness with reinforcement.

In general, the overall damping capacity of the metal matrix composite is directly related to the damping capacity of each of its constituents. Based on the literature review, Ti can exhibit a maximum loss factor of 0.003 [10] in the same range as that of aluminium, which is around 0.0032, based on the present work. Hence it can be expected that addition of Ti in the Al matrix would not result in any increase of the composite's damping capacity. Thus, the damping improvement observed from the experiment results has to be attributed primarily to the interface between reinforcement and the metallic matrix. In metallic materials the damping capacity arises due to intrinsic dissipation of strain energy due to mechanisms at the crystal level. The most significant role comes from point defect relaxation, microplasticity, dislocation motion, grain boundary sliding, inclusion-matrix friction, magnetoelastic effects,

TABLE III Results of theoretical predictions of microstructural characteristics and of experimental damping measurement

Ti weight(%)	Ti volume (%)	Interparticle spacing (μm)	Estimated plastic zone vol. fraction (%)	Estimated dislocation density (m^{-2})	Exp. damping loss factor η_{free}	Damping increase^{+} (%)	Dynamic modulus (GPa)
0.0	0	–	0.00	–	0.00322	–	68.39
3.3	1.8	38.46	8.61	7.9E + 11	0.00341	6	74.75
6	3.7	19.32	17.70	2.3E + 12	0.00376	17	78.01
7.5	5	27.86	23.92	1.9E + 12	0.00397	24	79.26

$^{+}$When compared to that of the monolithic sample.

and elastothermodynamic effects [10, 14–16]. Particulate reinforced metal matrix composites have additional mechanisms apart from the regular damping mechanisms in the metallic matrix due to a high residual stress in the matrix and due to high dislocation density at the particulate/matrix interface, which improve their damping capacity [16]. The high residual stresses and the dislocation density are caused due to large difference in the coefficient of thermal expansion between the phases (such as the CTE for Ti is 8.41 ppm/°C [17], and for Al is 25.2 ppm/°C, refer Table I). In addition, transformation of Ti to Al-Ti intermetallics can enhance this residual stresses and dislocation density since the coefficient of thermal expansion of intermetallics can be expected to be much lower than the parent metals. This will increase the overall CTE mismatch when compared to a pure Ti condition. To obtain a lower bound of this increase in dislocation density and residual stress at the particulate-matrix interface, the particulate can be considered to be pure Ti, as described in the forthcoming paragraphs. This increase in plasticity can be suspected to be one of the reasons behind the increase in microhardness value at the interface compared to the bulk matrix, listed in Table 1, as a result of strain hardening effect. This correlation of plastic zone to the microhardness is confirmed in reference [18] using X-ray diffraction analysis for a particulate reinforced Al composite.

Based on the works of Dunand and Mortensen [19], the high residual stresses results as an annular plastic zone of radius C_s around a spherical particle of radius r_s as follows:

$$C_s = r_s\left(\frac{\Delta\alpha E \Delta T}{(1-\nu)\sigma_y}\right) \tag{9}$$

where $\Delta\alpha$ is the difference between the CTEs of Al and Ti, ΔT is the temperature difference which is around 327°C, E and ν are the matrix elastic modulus and poisson's ratio, σ_y is the matrix yield stress and r_s is the particulate radius. Based on mechanical spectroscopic studies of Carreno-Morelli, Urreta and Schaller the damping due to plastic zone is as follows [20]:

$$\tan\phi \approx \frac{f_{zp} G_c \oint \sigma \, d\varepsilon}{\pi \sigma_o^2} \tag{10}$$

where f_{zp} is the plastic zone volume fraction, G_c is the shear modulus of the composite sample, σ_o is the maximum alternating shear stress amplitude, σ and ε is the corresponding stress and strain, respectively, acting on the specimen. Thus it is clear from Equation 10 that the damping depends directly on the strain amplitude and the volume fraction of the plastic zone, which directly depends on reinforcement volume fraction. Also it is clear that the interaction of plastic zones is expected to be more when the plastic zone is larger with smaller inter-particulate distance. Table III lists the plastic zone volume fraction computed from the plastic zone radius and the inter-particulate distance for the composite samples based on the model of Nardone and Prewo described as follows [21]:

$$\lambda = \left[\frac{lt}{V_f}\right]^{0.5} \tag{11}$$

where λ is the inter-particulate spacing, t, l and V_f are the thickness, length and volume fraction of the reinforcement, respectively. This also suggests that the presence of clusters which is random phenomena can result in over-lapping of thermal-mismatch induced plastic zones and thus affect the overall plastic zone within the sample. Secondly, the overall stiffness or the elastic modulus of the composite decreases due to the presence of clusters and hence the maximum strain energy per unit volume that the composite can sustain also decreases. In addition presence of porosity within a cluster may further affect the cluster's dynamic rigidity and damping capacity.

Another major source of damping can be expected due to the high dislocation density ρ_{th} at the particle-matrix interface, which are listed in Table III. These were computed using the prismatic dislocation-punching model of Arsenault and Shi model expressed as follows [22]:

$$\rho_{th} = \frac{B\Delta\alpha\Delta T V_f}{bt(1-V_f)} \tag{12}$$

where B is a geometric constant (equals 12 for equiaxed particulates), b the Burgers vector which is around 0.3 nm [23], and t is the smallest dimension of the reinforcement.

According to Granato-Lucke dislocation model, the dislocation behaves like an elastic string pinned between both sides due to any hard particulates such as precipitates, reinforcement particulate or antiplane dislocations and under a low strain amplitude (below 10^{-4}) type cyclic load it bows, which introduces increased relative atomic movement in a crystalline lattice thus interfering with homogenous deformation of the bulk material [10, 24]. In the present experimental setup the strain magnitude induced in the specimen is of the order of 10^{-6} and hence the frequency dependent dislocation

damping is applicable and is as follows [24]:

$$Q_{\mathrm{f}}^{-1} \approx \frac{a_{\mathrm{o}} B \Lambda L^4 \omega^2}{\pi^2 C b^2} \tag{13}$$

where a_{o} is a numerical factor of order l, B is the damping constant, ω is the operating frequency, L is the effective dislocation loop length which depends on the pinning distance, C is the dislocation line tension ($\approx 0.5Gb^2$), G is the shear modulus, b is burgers vector and Λ is the total dislocation density. Thus increased density of dislocation due to presence of Ti and its intermetallics in the Al matrix contributes to increased dislocation-based damping characteristics in the MMC. Experiment results in Table III shows an increase in damping factor when the particulate weight percentage increases which confirms this hypothesis.

Furthermore, from Table I it is clear that the hardness of the Ti reinforced samples is in general higher than that of unreinforced material. Table I also shows increased hardness at the interface than in the metallic matrix at a location away from the interface in any Ti containing composite, which can partly be attributed to the accumulation of residual plastic zone due to thermal mismatch at the particulate-matrix interface, dislocation density and reduction in grain size. XRD results performed at the particle-matrix interface shows the presence of Al-Ti intermetallics as well as oxides. Their presence at the particulate-matrix interface can be expected to result in increased plastic zone radius due to increased CTE mismatch, since intermetallics and oxides are expected to have lower CTE compared to their parent materials.

Other damping mechanisms such as grain boundary sliding and elasto-thermodynamic damping can be seen to be insignificant in the present experimental study due to room temperature operation conditions, sample dimensions and frequency magnitude [15, 25, 26].

Thus from the above discussions, it is encouraging to note that addition of stiffer metallic phase in the form of particulates in a metallic matrix increases both modulus and damping reasonably. Presently, further work is in progress on other composite formulations to further strengthen the feasibility of this approach.

5. Conclusions

1. The free-free beam type flexural resonance method can successfully be used with circle-fit approach to measure the stiffness and damping characteristics of the Al-Ti metastable composites.

2. Addition of Ti particulates in a metal matrix enhances energy dissipation due to the various intrinsic damping mechanisms acting parallel.

3. Experiment results show that damping of Al increases with an increase in Ti weight percentage. This can be explained due to increase in dislocation density and plastic zone radius.

4. An increase in the weight percentage of Ti particulates in the aluminium matrix increases the elastic modulus of the composite material.

Acknowledgements

The authors wish to acknowledge NUS RP (R-265-000-142-112) for financial support towards the research work.

References

1. R. B. BHAGAT, "Damping of Multiphase Inorganic Materials" ASM International (Materials Park, Ohio, USA, 1993).
2. N. SRIKANTH, L. M. THAM and M. GUPTA, *Alumin. Trans.* **1** (1999) 11.
3. N. SRIKANTH and M. GUPTA, *Key Engng. Mater.* **227** (2002) 211.
4. N. SRIKANTH, V. V. GANESH and M. GUPTA, *Mat. Sci. and Tech.* **19** (2003) 1.
5. A. MANNA and B. BATTACHARAYYA, *Mater. Proc. Techn.* **140** (2003) 711.
6. M. GUPTA, J. JUAREZ-ISLAS, W. E. FRAZIER, F. A. MOHAMED and E. J. LAVERNIA, *Metall. Trans. B* **23** (1992) 719.
7. A. BUCH, "Pure Metals Properties—A Scientific Technical Handbook" (ASM International, Materials Park, Ohio, USA, 1999).
8. ASTM C1259-98: 'Dynamic Young's Modulus, Shear modulus, and Poisson's Ratio for Advanced Ceramics by Impulse Excitation of Vibration,' Annual Book of ASTM Standards, 1998 (American Society for Testing and Materials, Philadelphia, 1998) p. 1.
9. D. J. EWINS, "Modal Testing: Theory and Practice" (Research Studies Press, New York, 1984).
10. B. J. LAZAN, "Damping of Materials and Members in Structural Mechanics" (Pergamon Press, New York, 1968).
11. S. L. CHEN ZHANG, Y. A. CHANG and U. R. KATTNER, *Intermetallics* **5** (1997) 471.
12. M. GUPTA, F. Y. CHUNG and T. S. SRIVATSAN, *Mater. Manufact. Proc.* **18**(6) (2003) 891.
13. L. M. PENG, J. H. WANG, H. LI, J. H. ZHAO and L. H. HE, *Scripta Materialia* **52** (2004) 243.
14. R. D. BATIST, in "Materials Science and Technology—A Comprehensive Treatment," Vol. 2b, Characterization of Materials part II, edited by. R. W. Cahn, P. Haasen and E. J. Kramer (VCH Publishers, New York, 1994) p. 161.
15. J. E. BISHOP and V. K. KINRA. *Metall. Mater. Trans. A* **26A** (1995) 2773.
16. R. B. BHAGAT, M. F. AMATEAU and E. C. SMITH, *Intern. J. Powder Metall.* **25** (1986) 311.
17. M. J. DONACHIE, "Titanium—A Technical Guide" (ASM International, Materials Park, Ohio, USA, 2000) p. 6.
18. S. K. SHEE, S. K. PRADHAN and M. DE, *Mater. Chem. Phy.* **52** (1998) 228.
19. D. DUNAND and A. MORTENSEN, *Mater. Sci. Engng.* **A135** (1991) 179.
20. E. CARRENO-MORELLI, S. E. URRETA and R. SCHALLER, *Acta Mater.* **48** (2000) 4725.
21. V. C. NARDONE and K. W. PREWO, *Scr. Metall.* **20** (1986) 43.
22. T. MINORO and R. J. ARSENAULT, "Metal Matrix Composites—Thermomechanical Behavior" (Pergamon Publishers, New York, USA, 1989).
23. H. J. FROST and M. F. ASHBY, "Deformation-Mechanism Maps: The Plasticity and Creep of Metals and Ceramics" (Pergamon Press, Oxford, New York, 1982).
24. A. GRANATO and K. LUCKE, *J. Appl. Phy.* **27** (1956) 583.
25. T. S. KÊ. *Phys. Rev.* **71** (1947) 533.
26. E. J. LAVERNIA, R. J. PEREZ and J. ZHANG, *Metall. Mater. Trans. A* **26A** (1995) 2803.

Received 24 September
and accepted 20 December 2004